A&A 457, 637–644 (2006)
DOI: 10.1051/0004-6361:20065753

Astronomy & Astrophysics

UBVJHK synthetic photometry of Galactic O stars⋆

F. Martins[1] and B. Plez[2]

[1] Max-Planck Institut für Extraterrestrische Physik, Postfach-1312, 85741 Garching, Germany
e-mail: martins@mpe.mpg.de
[2] GRAAL, CNRS UMR 5024, Université Montpellier II, 34095 Montpellier Cedex 5, France
e-mail: bertrand.plez@graal.univ-montp2.fr

Received 2 June 2006 / Accepted 14 June 2006

ABSTRACT

Aims. The development of powerful infrared observational techniques enables the study of very extincted objects and young embedded star-forming regions. This is especially interesting in the context of massive stars that form and spend a non negligible fraction of their life still enshrouded in their parental molecular cloud. Spectrophotometric calibrations are thus necessary to constrain the physical properties of heavily extincted objects.
Methods. Here, we derive *UBVJHK* magnitudes and bolometric corrections from a grid of atmosphere models for O stars. Bessel passbands are used. Bolometric corrections (BC) are derived as a function of $T_{\rm eff}$ and are subsequently used to derive BC-spectral type (ST) and absolute magnitudes-ST relations.
Results. Infrared magnitudes and, for the first time, bolometric corrections are given for the full range of spectral types and luminosity classes. Infrared colors are essentially constant, and $(H-K)_0$ is 0.05 mag bluer than previously proposed. Optical calibrations are also provided and are similar to previous work, except for $(B-V)_0$ which is found to be at minimum −0.28 for standard O stars, slightly higher (0.04 mag) than commonly accepted.
Conclusions. We present a consistent set of photometric calibrations of optical and infrared magnitudes and bolometric corrections for Galactic O stars as a function of $T_{\rm eff}$ and spectral type based on non-LTE atmosphere models including winds and line-blanketing.

Key words. stars: fundamental parameters – stars: atmospheres – stars: early-type

1. Introduction

Massive stars are known to play an important role in various fields of astrophysics, from stellar physics to ISM studies and the chemical evolution of galaxies, through cosmological issues, such as the reionisation of the Universe. In particular, the connection between massive stars and star formation is very tight. As a result of their short lifetimes, massive stars are associated with star forming events, and their feedback effects (radiation, winds) have a strong impact on star formation processes. Moreover, their ionising fluxes are responsible for nebular emission lines such as Ly_α or H_α, two lines usually used to trace star formation (Kennicutt 1998; Russeil et al. 2005). However, the details of the formation of *individual* massive stars is still a matter of debate: a standard accretion process deals with the problem of the strong radiative pressure generated by the luminosity of young massive proto-stars, so that the mass growth can be stopped at around 10 $M_\odot$. Although progress has been recently made (Yorke & Sonnhalter 2002; Krumholz et al. 2005), another scenario in which massive stars form through mergers of low mass protostars in dense clusters was proposed by Bonnell et al. (1998). This key question of the formation of the most massive stars has triggered a number of observational studies aimed at obtaining constraints on the properties of the youngest objects (e.g. Crowther & Conti 2004; Bik et al. 2005). Due to the short evolutionary timescale of massive stars, heavily extincted young star forming regions have to be probed, which requires the use of infrared spectrophotometry.

Although in principle using only spectroscopy allows a derivation of spectral types and luminosity classes (LC), photometry can be useful. This is the case when spectra have to be corrected for nebular emission always present in star forming regions, rendering the line strength/shape uncertain. As a result, spectral classification and luminosity classes determinations are difficult. Moreover the luminosity is usually derived from observed magnitudes, extinction and bolometric corrections. Estimates of extinction often rely on the intrinsic colors of stars, while the knowledge of bolometric corrections requires atmosphere models, so that accurate intrinsic photometry is crucial for getting access to luminosities. Although such photometry is usually available in the optical range (Kurucz 1979; Schmidt-Kaler 1982; Conti et al. 1986), this is not the case in the infrared where calibrations are incomplete. The widely-used intrinsic colors of Koorneef (1983) are only given for O6 to O9.5 dwarfs and the latest O supergiants. Johnson (1966) covers the same range of spectral types/luminosity class.

In this context, the recent development of reliable atmosphere models for massive stars is certainly welcome. Indeed, including line-blanketing in such models now allows realistic prediction of atmospheric structures and emergent spectra that are being used to quantitatively constrain the properties of massive stars (Crowther et al. 2002; Hillier et al. 2003; Bouret et al. 2003; Martins et al. 2004; Repolust et al. 2004; Martins et al. 2005b). The grid of models computed by Martins et al. (2005a, herafter MSH05) and the associated SEDs are especially interesting since they can be used to compute optical and, most

⋆ Tables 2 and 3 are also available in electronic form at the CDS via anonymous ftp to cdsarc.u-strasbg.fr (130.79.128.5) or via http://cdsweb.u-strasbg.fr/cgi-bin/qcat?J/A+A/457/637

important, near-infrared photometry for the whole range of O stars. Together with effective temperature scales, calibrations of magnitudes and bolometric corrections as a function of spectral type can thus be produced.

In this paper, we used the SEDs of MSH05 to calculate *UBVJHK* photometry. In Sect. 2 we present our method and give the results that are discussed in Sect. 3 and summarized in Sect. 4.

2. Synthetic photometry

We first present our method to calculate *UBVJHK* photometry and to produce the various calibrations (Sect. 2.1). We then discuss the uncertainties of our results in Sect. 2.2.

2.1. Method and results

Synthetic photometry was computed from the grid of atmosphere models presented by Martins et al. (2005a)[1]. From the emergent SED (flux per unit of star surface, F_λ) we computed the magnitude in each band

$$M_\lambda = -2.5 \times \log \int F_\lambda B_\lambda \mathrm{d}\lambda + \mathrm{const.} \quad (1)$$

with B_λ the filter passband, according to Bessel et al. (1998). Photometry is thus computed in the *UBV* passbands defined by Bessel (1990, Johnson-Cousins system) and in the *JHK* passbands of Bessel & Brett (1988, Johnson-Glass system) for the near-IR.

Once obtained, these magnitudes were subsequently used to determine bolometric corrections for each band from

$$BC_\lambda = M_\odot^{\mathrm{bol}} - M_\lambda - 2.5 \times \log\left(\frac{L}{L_\odot}\right) \quad (2)$$

where BC_λ is the associated bolometric correction, $M_\odot^{\mathrm{bol}}$ is the bolometric magnitude of the sun taken to be equal to 4.75 (recommendation of IAU 1999), and L is the luminosity. Thus, BC_λ is computed for each model so that we have bolometric corrections for the whole range of effective temperatures of O stars. These values are shown in Fig. 1 where we see that there is a tight correlation between BC_λ and $\log T_{\mathrm{eff}}$ for each band. A simple linear regression of the form

$$BC_\lambda = A \times \log(T_{\mathrm{eff}}) + B \quad (3)$$

gives the calibration between BC_λ and effective temperature. Parameters A and B of Eq. (3) are given in Table 1 together with the dispersion σ. The dispersion is larger in the infrared due to the increasing contribution of wind emission that introduces a scatter (see Sect. 2.2).

The T_{eff}-scales of MSH05 for various luminosity classes were subsequently used to convert effective temperatures into spectral types, leading to the calibration of bolometric corrections as a function of spectral type. The results of this simple conversion using the "observational" T_{eff}-scale of MSH05 are shown in Fig. 2 for dwarf stars.

Finally, using these new $BC_\lambda - ST$ calibrations, the relations between $\log \frac{L}{L_\odot}$ and ST of MSH05 and Eq. (2), we can estimate the absolute magnitude in all bands for each spectral type and luminosity classes: we obtain the $M_\lambda - ST$ relations (Fig. 2 shows the relation for dwarf stars).

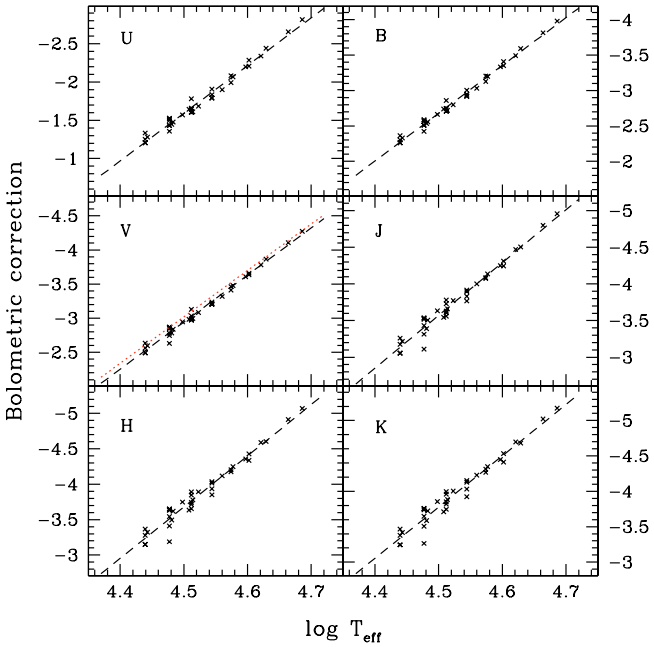

Fig. 1. Bolometric correction in different bands as a function of effective temperature for the models of MSH05 (crosses). The dashed lines are the regression curves (see Table 1 for the corresponding parameters). The red dotted line in the plot BC_{V}-T_{eff} plot is the relation given by MSH05.

To avoid any confusion, we want to stress that using Eq. (1) directly gives the absolute magnitudes for each model, and in principle inspection of the spectrum can also provide the spectral type. In practice, we then have M_λ and the spectral type for each model. However, we are interested here in producing calibrations $BC_\lambda - ST$ and $M_\lambda - ST$ for the three main luminosity classes (dwarfs, giants, and supergiants) that are defined by specific relations between $\log g$ and ST (see MSH05). Our models do not fall exactly on these relations, some being in between two luminosity classes (by construction of the grid). Hence, the approach adopted here is aimed at taking this into account and is well-suited to our purpose, namely producing calibrations for each luminosity class.

The results of the calibrations are gathered in Tables 2 and 3. In the former, the "observational" T_{eff} scale of MSH05 is used, while in the latter, we make use of their "theoretical" T_{eff}–ST relation. Inspection of Tables 2 and 3 reveals that adopting the "theoretical" T_{eff} scale of MSH05 changes the magnitudes very little: the differences are not larger than 0.03 mag. The conclusion is the same for bolometric corrections of the earliest spectral types, while later type stars suffer from larger differences (up to 0.22 mag). This is expected since late types are the ones for which the two effective temperature scales differ the most. Note that the colors are basically unaffected by the change of the effective temperature scale since they depend very little on T_{eff}. Since at present it is not clear which T_{eff}-scale better reflects the true properties of O stars, we chose to provide both calibrations.

2.2. Accuracy of calibrations

In Fig. 1 and Table 1, we see that the dispersions around the average $BC - T_{\mathrm{eff}}$ relation increases with wavelength. This is a natural consequence of the stronger sensitivity of the SED to wind

[1] Note that the spectral energy distributions of these models are available at the following URL `http://www.mpe.mpg.de/~martins/SED.html`

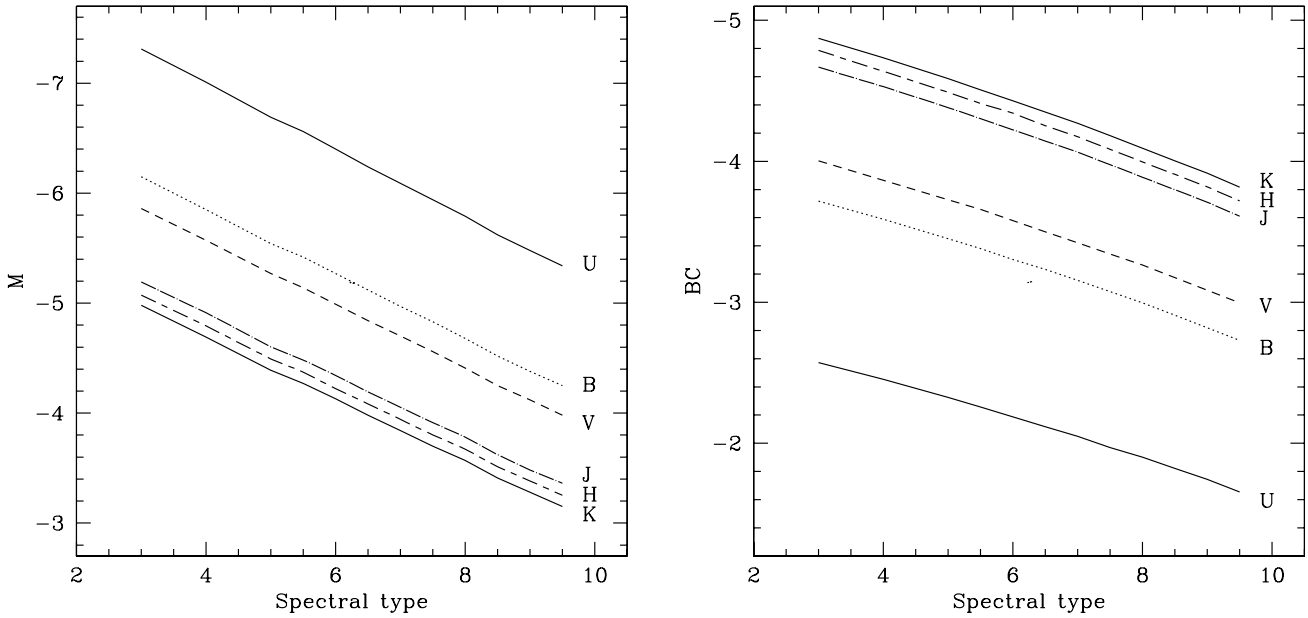

Fig. 2. Magnitudes (*left*) and bolometric corrections (*right*) as a function of spectral type for dwarf stars computed using the "observational" $T_{\rm eff}$-scale of MSH05.

Table 1. Parameters of the linear regression curves for the BC_λ–$T_{\rm eff}$ relations (A, B, see Eq. (3)) together with dispersion σ.

Band	A	B	σ
U	−6.23	26.46	0.05
B	−6.75	27.70	0.04
V	−6.89	28.07	0.05
J	−7.20	28.85	0.08
H	−7.24	28.89	0.09
K	−7.24	28.80	0.10

parameters at longer wavelengths. Indeed, massive stars are known to emit a significant excess of radiation in the IR-radio range due to free-free emission originating in their wind (e.g. Lamers & Cassinelli 1999). This is illustrated in Fig. 3, which shows the variation of the SED when the mass loss rate is increased by a factor of 3 (which is the typical uncertainty claimed by detailed analysis) in a model for an early supergiant. This reveals that any variation in the wind parameters will change the wind density, which in turn will affect both the continuum level and the strength of near IR emission lines (see Fig. 3), leading to a modification of the IR photometry. In order to estimate the magnitude of this effect, we ran test models[2] for a sample of stars for which the mass-loss rate was increased by a factor of 3. The results are gathered in Table 4. For such a change in wind density, the typical variation in bolometric correction is ~0.02 mag in U, while it can reach 0.2 mag in K. Note that this is similar to the dispersion of relation 3.

Figure 1 also shows the calibration of BC_V as a function of $T_{\rm eff}$ as obtained by MSH05. We see that it is slightly different from the one presented here, although it is based on the same models. The reason for this small discrepancy is the use of a fixed effective wavelength (5500 Å) in the computation of MSH05, while here we use filter curves providing a better measure of the flux in the V band. The corresponding new effective wavelengths are usually shorter than 5500 Å, leading to a slightly smaller magnitude and consequently to a slightly larger bolometric correction, as seen in Fig. 1. Recomputing photometry as in MSH05 with the more accurate effective wavelengths of the present study leads to excellent agreement with the magnitudes presented here (differences smaller than 0.01 mag).

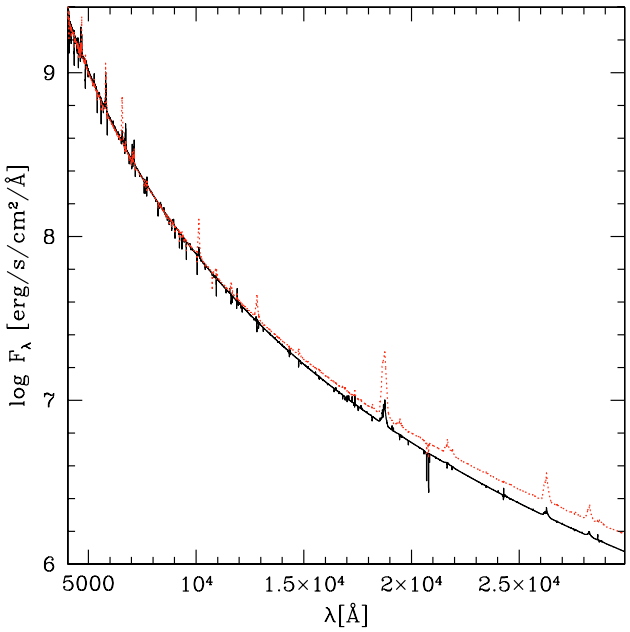

Fig. 3. Variation of the SED as a function of mass-loss rate: the black solid curve is for $\dot{M} = 1.32 \times 10^{-5}\ M_\odot\ {\rm yr}^{-1}$, while the red dotted line is for a mass-loss rate that is three times larger. The other parameters of the model are $T_{\rm eff} = 48\,530$ K, $\log g = 4.01$ and $v_\infty = 2977$ km s^{-1}.

[2] The parameters of the initial models are: $T_{\rm eff} = 32\,210$ K, $\log g = 3.26$, $\dot{M} = 10^{-4.93}\ M_\odot\ {\rm yr}^{-1}$, $v_\infty = 1960$ km s^{-1} for model A1, $T_{\rm eff} = 33\,340$ K, $\log g = 4.01$, $\dot{M} = 10^{-6.86}\ M_\odot\ {\rm yr}^{-1}$, $v_\infty = 2544$ km s^{-1} for model B1, $T_{\rm eff} = 42\,560$ K, $\log g = 3.71$, $\dot{M} = 10^{-4.88}\ M_\odot\ {\rm yr}^{-1}$, $v_\infty = 2538$ km s^{-1} for model C1, $T_{\rm eff} = 48\,530$ K, $\log g = 4.01$, $\dot{M} = 10^{-5.38}\ M_\odot\ {\rm yr}^{-1}$, $v_\infty = 2977$ km s^{-1} for model D1.

Table 2. Optical and infrared magnitudes, colors and bolometric corrections of O stars derived using the "observational" $T_{\rm eff}$-scale of MSH05.

ST	M_U	M_B	M_V	M_J	M_H	M_K	$(U-B)_0$	$(B-V)_0$	$(J-H)_0$	$(H-K)_0$	BC_U	BC_B	BC_V	BC_J	BC_H	BC_K
O3V	−7.31	−6.15	−5.86	−5.19	−5.07	−4.98	−1.16	−0.28	−0.11	−0.10	−2.54	−3.70	−3.99	−4.66	−4.78	−4.87
O4V	−7.01	−5.85	−5.57	−4.91	−4.79	−4.69	−1.15	−0.28	−0.11	−0.10	−2.42	−3.57	−3.85	−4.52	−4.63	−4.73
O5V	−6.69	−5.54	−5.27	−4.60	−4.49	−4.39	−1.14	−0.28	−0.11	−0.10	−2.29	−3.43	−3.71	−4.37	−4.48	−4.58
O5.5V	−6.56	−5.42	−5.14	−4.48	−4.37	−4.27	−1.14	−0.28	−0.11	−0.10	−2.22	−3.36	−3.64	−4.29	−4.40	−4.50
O6V	−6.40	−5.27	−4.99	−4.34	−4.22	−4.13	−1.13	−0.28	−0.11	−0.10	−2.15	−3.28	−3.56	−4.21	−4.33	−4.42
O6.5V	−6.24	−5.12	−4.84	−4.19	−4.08	−3.98	−1.13	−0.27	−0.11	−0.10	−2.08	−3.21	−3.48	−4.13	−4.24	−4.34
O7V	−6.09	−4.97	−4.70	−4.05	−3.94	−3.84	−1.12	−0.27	−0.11	−0.10	−2.01	−3.13	−3.40	−4.05	−4.16	−4.26
O7.5V	−5.94	−4.83	−4.56	−3.91	−3.80	−3.70	−1.11	−0.27	−0.11	−0.10	−1.93	−3.05	−3.32	−3.96	−4.07	−4.17
O8V	−5.79	−4.68	−4.41	−3.78	−3.67	−3.57	−1.11	−0.27	−0.11	−0.10	−1.86	−2.97	−3.24	−3.87	−3.98	−4.08
O8.5V	−5.62	−4.52	−4.25	−3.62	−3.51	−3.41	−1.10	−0.27	−0.11	−0.10	−1.78	−2.88	−3.15	−3.78	−3.89	−3.99
O9V	−5.48	−4.38	−4.12	−3.48	−3.38	−3.28	−1.10	−0.27	−0.11	−0.10	−1.70	−2.79	−3.06	−3.69	−3.80	−3.90
O9.5V	−5.34	−4.25	−3.98	−3.36	−3.25	−3.15	−1.09	−0.26	−0.11	−0.10	−1.61	−2.70	−2.97	−3.59	−3.70	−3.80
O3III	−7.63	−6.47	−6.18	−5.51	−5.40	−5.30	−1.16	−0.28	−0.11	−0.10	−2.52	−3.68	−3.97	−4.64	−4.75	−4.85
O4III	−7.49	−6.33	−6.05	−5.39	−5.27	−5.18	−1.15	−0.28	−0.11	−0.10	−2.39	−3.54	−3.82	−4.49	−4.60	−4.70
O5III	−7.33	−6.18	−5.91	−5.25	−5.14	−5.04	−1.14	−0.28	−0.11	−0.10	−2.25	−3.39	−3.67	−4.33	−4.44	−4.54
O5.5III	−7.25	−6.11	−5.84	−5.18	−5.07	−4.97	−1.14	−0.28	−0.11	−0.10	−2.18	−3.31	−3.59	−4.24	−4.36	−4.46
O6III	−7.17	−6.04	−5.77	−5.12	−5.00	−4.91	−1.13	−0.27	−0.11	−0.10	−2.10	−3.23	−3.51	−4.16	−4.27	−4.37
O6.5III	−7.07	−5.95	−5.68	−5.03	−4.92	−4.82	−1.12	−0.27	−0.11	−0.10	−2.03	−3.15	−3.42	−4.07	−4.18	−4.28
O7III	−7.00	−5.88	−5.61	−4.97	−4.86	−4.76	−1.12	−0.27	−0.11	−0.10	−1.95	−3.07	−3.34	−3.98	−4.09	−4.19
O7.5III	−6.93	−5.82	−5.55	−4.91	−4.80	−4.70	−1.11	−0.27	−0.11	−0.10	−1.87	−2.98	−3.25	−3.89	−4.00	−4.10
O8III	−6.84	−5.74	−5.47	−4.83	−4.72	−4.62	−1.10	−0.27	−0.11	−0.10	−1.79	−2.89	−3.16	−3.79	−3.90	−4.00
O8.5III	−6.75	−5.65	−5.39	−4.76	−4.65	−4.55	−1.10	−0.27	−0.11	−0.10	−1.70	−2.80	−3.06	−3.69	−3.80	−3.90
O9III	−6.66	−5.58	−5.31	−4.68	−4.58	−4.48	−1.09	−0.26	−0.11	−0.10	−1.61	−2.70	−2.96	−3.59	−3.70	−3.80
O9.5III	−6.60	−5.52	−5.26	−4.64	−4.53	−4.43	−1.08	−0.26	−0.11	−0.10	−1.52	−2.60	−2.86	−3.48	−3.59	−3.69
O3I	−7.85	−6.70	−6.42	−5.75	−5.64	−5.54	−1.15	−0.28	−0.11	−0.10	−2.38	−3.53	−3.81	−4.47	−4.59	−4.69
O4I	−7.82	−6.68	−6.40	−5.74	−5.63	−5.53	−1.14	−0.28	−0.11	−0.10	−2.26	−3.40	−3.68	−4.34	−4.45	−4.55
O5I	−7.79	−6.66	−6.39	−5.73	−5.62	−5.52	−1.13	−0.28	−0.11	−0.10	−2.13	−3.26	−3.54	−4.19	−4.30	−4.40
O5.5I	−7.78	−6.66	−6.38	−5.73	−5.62	−5.52	−1.13	−0.27	−0.11	−0.10	−2.07	−3.19	−3.47	−4.12	−4.23	−4.33
O6I	−7.77	−6.65	−6.38	−5.73	−5.62	−5.52	−1.12	−0.27	−0.11	−0.10	−2.00	−3.12	−3.40	−4.04	−4.15	−4.25
O6.5I	−7.76	−6.65	−6.38	−5.74	−5.62	−5.53	−1.11	−0.27	−0.11	−0.10	−1.94	−3.05	−3.32	−3.96	−4.08	−4.17
O7I	−7.76	−6.65	−6.38	−5.74	−5.63	−5.53	−1.11	−0.27	−0.11	−0.10	−1.87	−2.98	−3.24	−3.89	−4.00	−4.09
O7.5I	−7.75	−6.65	−6.38	−5.75	−5.64	−5.54	−1.10	−0.27	−0.11	−0.10	−1.80	−2.90	−3.17	−3.80	−3.91	−4.01
O8I	−7.73	−6.63	−6.36	−5.73	−5.62	−5.52	−1.10	−0.27	−0.11	−0.10	−1.72	−2.82	−3.09	−3.72	−3.83	−3.93
O8.5I	−7.73	−6.64	−6.37	−5.74	−5.63	−5.53	−1.09	−0.26	−0.11	−0.10	−1.65	−2.74	−3.00	−3.63	−3.74	−3.84
O9I	−7.70	−6.62	−6.36	−5.73	−5.62	−5.52	−1.08	−0.26	−0.11	−0.10	−1.57	−2.66	−2.92	−3.54	−3.65	−3.75
O9.5I	−7.68	−6.61	−6.34	−5.72	−5.62	−5.52	−1.08	−0.26	−0.11	−0.10	−1.49	−2.57	−2.83	−3.45	−3.56	−3.66

In conclusion, we see that the accuracy of the magnitudes and bolometric corrections is usually better than 0.1 mag and reaches 0.2 mag in K band. In any case, this uncertainty is of the order of the difference between two spectral sub types within a luminosity class.

3. Comparison with previous studies

In this section, we compare our results with previous analysis, focusing first on absolute magnitudes (Sect. 3.1) and second on intrinsic colors (Sect. 3.2), for both the optical and near-infrared ranges.

3.1. Absolute magnitudes

In terms of infrared magnitudes, Blum et al. (2000) derived absolute K magnitudes for ZAMS O stars using evolutionary models (Schaller et al. 1992), $V-K$ from Koorneef (1983), and $BC_V - ST$ and $T_{\rm eff}$–ST relations of Vacca et al. (1996). The comparison between their results and our relation for dwarfs is displayed in Fig. 4. We see that our calibration is slightly brighter. Since we calibrated photometry for "normal" O stars, it is not surprising that the ZAMS K magnitudes given by Blum et al. (2000) are fainter, ZAMS stars being fainter than standard O dwarfs (Hanson et al. 1997; Niemela et al. 2006). Note that the difference between the two calibrations increases with spectral type, which is also what is seen when comparing the position of standard O stars to the ZAMS in a HR diagram (e.g. Fig. 12 in MSH05). One could also argue that the use of different $T_{\rm eff}$-scales is responsible for the observed differences. However, this is not the case: had we used the same approach as Blum et al. (2000) to derive K magnitudes of ZAMS stars, but using the recent $T_{\rm eff}$ scale of MSH05, we would have found *fainter* K magnitudes than they find. Indeed, for a given ZAMS evolutionary model, i.e. for a given $T_{\rm eff}$ and luminosity, BC_V is similar if we use the Vacca et al. (1996) BC_V–$T_{\rm eff}$ calibration or the present one (similar to MSH05 too). The difference in bolometric corrections is less than 0.1 mag, so we would derive a similar V magnitude (within 0.1 mag) for the model. Using $V-K$ from Koorneef (1983) to get the K magnitude would then lead to a similar $M_{\rm K}$ (again within 0.1 mag). But now, using the recent $T_{\rm eff}$-scale of MSH05 instead of the one by Vacca et al. (1996, as in Blum et al. 2000) to convert $T_{\rm eff}$ into spectral type gives earlier values: the effective temperatures of MSH05 are indeed cooler for a given spectral type. This means that using the effective temperature calibrations of MSH05 instead of that of Vacca et al. (1996) translates to a shift of the $M_K - ST$ relation towards earlier spectral types. In that case, the difference with the calibration we provide in the present work is even higher. Hence, the use of different $T_{\rm eff}$-scales is not responsible for the shift seen in Fig. 4, which is more likely attributed to the different evolutionary status in the stars considered (ZAMS O stars versus "normal" O stars).

Table 3. Optical and infrared magnitudes, colors and bolometric corrections of O stars derived using the "theoretical" $T_{\rm eff}$-scale of MSH05.

ST	M_U	M_B	M_V	M_J	M_H	M_K	$(U-B)_0$	$(B-V)_0$	$(J-H)_0$	$(H-K)_0$	BC_U	BC_B	BC_V	BC_J	BC_H	BC_K
O3V	−7.30	−6.14	−5.85	−5.18	−5.07	−4.97	−1.16	−0.28	−0.11	−0.10	−2.52	−3.69	−3.97	−4.65	−4.76	−4.86
O4V	−7.00	−5.84	−5.56	−4.89	−4.78	−4.68	−1.16	−0.28	−0.11	−0.10	−2.45	−3.61	−3.89	−4.56	−4.67	−4.77
O5V	−6.69	−5.55	−5.27	−4.60	−4.49	−4.39	−1.15	−0.28	−0.11	−0.10	−2.33	−3.48	−3.76	−4.42	−4.53	−4.63
O5.5V	−6.54	−5.40	−5.12	−4.47	−4.35	−4.26	−1.14	−0.28	−0.11	−0.10	−2.23	−3.37	−3.65	−4.31	−4.42	−4.52
O6V	−6.40	−5.27	−5.00	−4.34	−4.23	−4.13	−1.13	−0.27	−0.11	−0.10	−2.10	−3.23	−3.50	−4.16	−4.27	−4.37
O6.5V	−6.25	−5.12	−4.85	−4.20	−4.09	−3.99	−1.12	−0.27	−0.11	−0.10	−2.00	−3.13	−3.40	−4.05	−4.16	−4.26
O7V	−6.09	−4.98	−4.71	−4.07	−3.96	−3.86	−1.11	−0.27	−0.11	−0.10	−1.91	−3.02	−3.29	−3.93	−4.04	−4.14
O7.5V	−5.93	−4.82	−4.55	−3.92	−3.81	−3.71	−1.11	−0.27	−0.11	−0.10	−1.82	−2.93	−3.20	−3.83	−3.94	−4.04
O8V	−5.76	−4.66	−4.40	−3.76	−3.65	−3.55	−1.10	−0.27	−0.11	−0.10	−1.74	−2.84	−3.10	−3.74	−3.85	−3.95
O8.5V	−5.63	−4.54	−4.27	−3.64	−3.53	−3.44	−1.09	−0.26	−0.11	−0.10	−1.67	−2.76	−3.03	−3.66	−3.77	−3.86
O9V	−5.47	−4.38	−4.12	−3.49	−3.38	−3.28	−1.09	−0.26	−0.11	−0.10	−1.58	−2.67	−2.93	−3.56	−3.67	−3.77
O9.5V	−5.31	−4.23	−3.97	−3.35	−3.24	−3.14	−1.08	−0.26	−0.11	−0.10	−1.49	−2.57	−2.83	−3.45	−3.56	−3.66
O3III	−7.63	−6.47	−6.19	−5.52	−5.41	−5.31	−1.16	−0.28	−0.11	−0.10	−2.42	−3.58	−3.86	−4.53	−4.64	−4.74
O4III	−7.47	−6.33	−6.05	−5.38	−5.27	−5.17	−1.15	−0.28	−0.11	−0.10	−2.33	−3.47	−3.75	−4.42	−4.53	−4.63
O5III	−7.30	−6.17	−5.89	−5.24	−5.12	−5.02	−1.14	−0.28	−0.11	−0.10	−2.20	−3.33	−3.61	−4.26	−4.38	−4.48
O5.5III	−7.23	−6.11	−5.83	−5.18	−5.07	−4.97	−1.13	−0.27	−0.11	−0.10	−2.09	−3.22	−3.49	−4.14	−4.25	−4.35
O6III	−7.16	−6.04	−5.76	−5.12	−5.01	−4.91	−1.12	−0.27	−0.11	−0.10	−1.99	−3.11	−3.39	−4.03	−4.14	−4.24
O6.5III	−7.06	−5.95	−5.67	−5.03	−4.92	−4.82	−1.11	−0.27	−0.11	−0.10	−1.92	−3.03	−3.30	−3.94	−4.05	−4.15
O7III	−6.99	−5.88	−5.61	−4.97	−4.86	−4.76	−1.11	−0.27	−0.11	−0.10	−1.84	−2.95	−3.21	−3.85	−3.96	−4.06
O7.5III	−6.90	−5.80	−5.54	−4.90	−4.79	−4.69	−1.10	−0.27	−0.11	−0.10	−1.75	−2.85	−3.11	−3.75	−3.86	−3.96
O8III	−6.83	−5.73	−5.47	−4.84	−4.73	−4.63	−1.09	−0.26	−0.11	−0.10	−1.67	−2.77	−3.03	−3.66	−3.77	−3.87
O8.5III	−6.75	−5.66	−5.40	−4.77	−4.67	−4.57	−1.09	−0.26	−0.11	−0.10	−1.60	−2.69	−2.95	−3.58	−3.68	−3.78
O9III	−6.66	−5.58	−5.32	−4.70	−4.59	−4.49	−1.08	−0.26	−0.11	−0.10	−1.52	−2.60	−2.86	−3.48	−3.59	−3.69
O9.5III	−6.58	−5.50	−5.24	−4.62	−4.51	−4.42	−1.08	−0.26	−0.11	−0.10	−1.47	−2.55	−2.81	−3.43	−3.54	−3.63
O3I	−7.85	−6.70	−6.42	−5.75	−5.64	−5.54	−1.15	−0.28	−0.11	−0.10	−2.40	−3.55	−3.83	−4.50	−4.61	−4.71
O4I	−7.82	−6.68	−6.40	−5.74	−5.63	−5.53	−1.14	−0.28	−0.11	−0.10	−2.28	−3.42	−3.70	−4.36	−4.47	−4.57
O5I	−7.80	−6.67	−6.39	−5.74	−5.63	−5.53	−1.13	−0.28	−0.11	−0.10	−2.13	−3.26	−3.53	−4.19	−4.30	−4.40
O5.5I	−7.78	−6.66	−6.38	−5.73	−5.62	−5.52	−1.12	−0.27	−0.11	−0.10	−2.02	−3.14	−3.42	−4.07	−4.18	−4.28
O6I	−7.78	−6.66	−6.39	−5.75	−5.64	−5.54	−1.11	−0.27	−0.11	−0.10	−1.92	−3.04	−3.31	−3.95	−4.06	−4.16
O6.5I	−7.76	−6.65	−6.38	−5.75	−5.64	−5.54	−1.11	−0.27	−0.11	−0.10	−1.84	−2.95	−3.22	−3.85	−3.96	−4.06
O7I	−7.74	−6.64	−6.38	−5.74	−5.63	−5.53	−1.10	−0.27	−0.11	−0.10	−1.73	−2.83	−3.10	−3.73	−3.84	−3.94
O7.5I	−7.73	−6.64	−6.38	−5.75	−5.64	−5.55	−1.09	−0.26	−0.11	−0.10	−1.62	−2.71	−2.97	−3.60	−3.71	−3.80
O8I	−7.71	−6.63	−6.37	−5.74	−5.63	−5.54	−1.08	−0.26	−0.11	−0.10	−1.54	−2.62	−2.88	−3.51	−3.62	−3.71
O8.5I	−7.70	−6.63	−6.37	−5.74	−5.64	−5.54	−1.08	−0.26	−0.11	−0.10	−1.50	−2.57	−2.83	−3.46	−3.56	−3.66
O9I	−7.69	−6.62	−6.36	−5.74	−5.63	−5.54	−1.07	−0.26	−0.11	−0.10	−1.41	−2.48	−2.74	−3.36	−3.47	−3.56
O9.5I	−7.67	−6.61	−6.35	−5.74	−5.63	−5.53	−1.06	−0.26	−0.11	−0.10	−1.30	−2.37	−2.62	−3.24	−3.34	−3.44

Calibrations of the V magnitudes as a function of spectral type have been discussed in MSH05 (see their Sect. 5.1): reasonable agreement with previous calibrations (differences smaller than 0.4 mag) was found. Inspection of Tables 2 and 3 together with Tables 1–6 of MSH05 reveals that the present V magnitudes are systematically smaller by 0.02–0.08 mag, which is simply due to the better computation of the V band photometry in the present study as discussed in Sect. 2.2. This difference is, however, well within the typical uncertainty of the calibrations.

3.2. Intrinsic colors

3.2.1. Optical range

Figure 5 shows the relation $(B-V)_0 - T_{\rm eff}$ from two sets of atmosphere models: the CMFGEN[3] models of MSH05 and Kurucz models (Kurucz 1979). On average and for a given $T_{\rm eff}$, it seems that the new colors are slightly redder, and that the dispersion is larger too. However, this can be explained simply by the effect of gravity. As shown by Abbott & Hummer (1985, and confirmed here), the SED of O stars depends on $\log g$, because when gravity decreases, the optical flux distributions get redder. This is clearly shown in Fig. 5 where, for a given $T_{\rm eff}$, a clear sequence of bluer $(B-V)_0$ appears when $\log g$ is increased[4]. The range of $\log g$ covered by the Kurucz models is 3.50–5.00, while the grid of MSH05 has $3.20 < \log g < 4.25$ (see coding in Fig. 5). Thus on average, redder $(B-V)_0$ are naturally expected for these new models (as seen in Fig. 5). The models of MSH05 also do not reach very blue colors, since they are restricted to lower gravities compared to the Kurucz models. It is also worth noting that the CMFGEN models include winds, which are know to affect the SED (see Sect. 2.2, and Gabler et al. 1989). However, the effects are reduced in the optical range. A simple inspection of Table 4 reveals that increasing the mass-loss rate by a factor 3 leads to changes in $B-V$ (equal to $BC_V - BC_B$ for a given model) by no more than 0.1 mag. Consequently, the redder colors observed in Fig. 5 for the new models can be safely attributed to lower $\log g$.

Table 4. Bolometric corrections of models with $\dot{M}$ increased by a factor of 3 (A2, B2, C2, D2) compared to initial models (A1, B1, C1, D1).

	BC_U	BC_B	BC_V	BC_J	BC_H	BC_K
A1	−1.644	−2.738	−2.984	−3.544	−3.636	−3.712
A2	−1.654	−2.750	−3.006	−3.519	−3.588	−3.607
B1	−1.685	−2.799	−3.085	−3.773	−3.893	−4.003
B2	−1.685	−2.800	−3.087	−3.776	−3.892	−3.999
C1	−2.442	−3.592	−3.865	−4.506	−4.603	−4.681
C2	−2.460	−3.609	−3.881	−4.441	−4.500	−4.496
D1	−2.815	−3.980	−4.272	−4.958	−5.071	−5.174
D2	−2.806	−3.980	−4.268	−4.941	−5.039	−5.115

[3] For more details on the models, see Hillier & Miller (1998).

[4] Note, however, that deviations to this general trend appear for the models at low $T_{\rm eff}$.

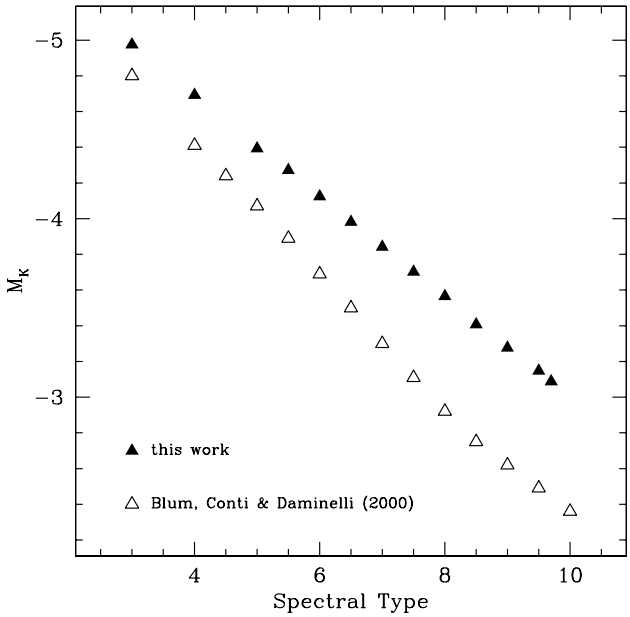

Fig. 4. Absolute K magnitudes as a function of spectral types for dwarfs. Filled triangles are this work, while open triangles are the calibration of Blum et al. (2000). The difference is mostly due to the fact that Blum et al. (2000) give parameters for ZAMS stars while we provide calibration for "normal" O dwarfs.

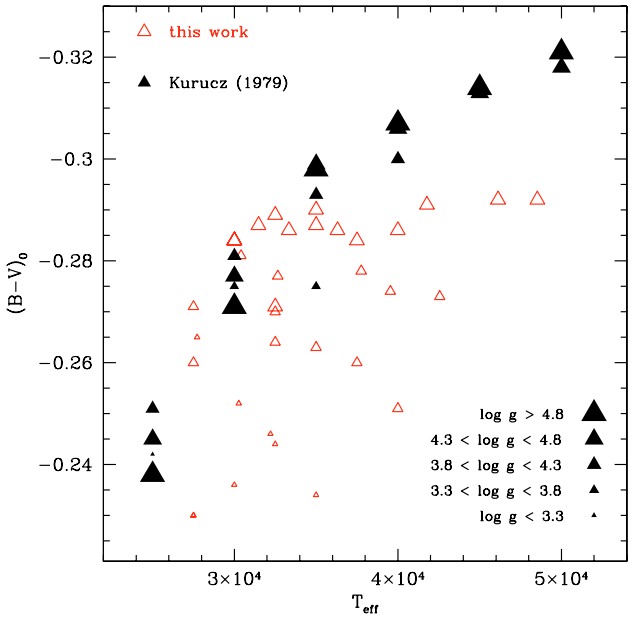

Fig. 5. $(B-V)_0$ as a function of effective temperature for the present work (red open triangles) and from Kurucz (1979) (black full triangles). For the present work, $(B-V)_0$ have been computed from the original grid of models and are not taken directly from Tables 2 and 3. The size of the symbols scales with $\log g$ (bigger symbols corresponding to higher gravities).

Further inspection of Tables 2 and 3 reveals that for standard O stars of any spectral type/luminosity class, $(B-V)_0$ *is never bluer than* -0.28. This is because normal O stars have well-defined $\log g - ST$ relations for which $\log g$ never exceeds ∼4.0 (see e.g. Fig. 2 in MSH05). Again, this does not mean that very blue (lower than −0.30) $(B-V)_0$ colors cannot be obtained with atmosphere models, but this requires very large gravities ($\log g > 4.25$), which are not typical of normal O stars (but probably more of very young massive stars).

How does this result compare to previous studies? Johnson (1966) derived $(B-V)_0 = -0.30/-0.32$ for O5–O9.5 stars fitting the envelope of the position of O stars in a two-color diagram (see his Fig. 1). This method assumes that the color is almost independent of spectral type (which is indeed the case), but Johnson uses a sample of stars covering only part of the range of spectral types (especially missing the earliest O stars), which may lead to uncertainties in the derived average values.

Fitzgerald (1970) also determined intrinsic colors of O stars using the method of the bluest envelope in a two-color diagram, but he adopted $(B-V)_0 = -0.32$ from Johnson (1963). This color was determined from studies of O stars in associations in which the color excess was determined from the photometry of later type stars.

Later, Conti et al. (1986) derived colors of early-type stars in the LMC and found $(B-V)_0 = -0.30$ for most O stars and $(B-V)_0 = -0.24$ for late supergiants. They also highlighted that the intrinsic colors in the LMC were slightly redder than in the Galaxy (while they should be similar or slightly bluer due to metallicity effects, see below), pointing to a possible problem with the Galactic reddening estimates and, consequently, with the Galactic intrinsic colors.

Fitzpatrick (1988) also studied OB supergiants in the LMC and derived $(B-V)_0 = -0.27$ for O3–6 stars and $(B-V)_0 = -0.23$ for O7–9.7 supergiants, stressing the variation in colors within the different O stars luminosity classes. Fitzpatrick (1988) also compared Strömgren and Johnson intrinsic colors in the Galaxy and LMC and again highlighted possible calibration uncertainties for the Galaxy.

We find $(B-V)_0 > -0.28$ for Galactic O stars. This is about 0.04 mag redder than the early results of Johnson (1966) and Fitzgerald (1970), but in reasonable agreement with the more recent study of Fitzpatrick (1988), although this study is based on LMC stars. We have not computed models at $Z = 0.5\ Z_\odot$ (typical of the LMC), but we do not expect changes in $(B-V)_0$ larger than ∼0.01 mag. Indeed, effective temperatures are expected to be larger – for a given spectral type – in low metallicity environments (see e.g. Mokiem et al. 2004; Massey et al. 2004), but examination of Tables 2 and 3 shows that $(B-V)_0$ is hardly sensitive to $T_{\rm eff}$ within the whole range of O stars, because it changes by no more than 0.02 mag. Hence, $(B-V)_0$ should be very similar in the LMC and in the Galaxy, which is confirmed by the good agreement between our results and those of Fitzpatrick (1988). Note, however, that we find $(B-V)_0$ is slightly bluer than Fitzpatrick (1988) for late supergiants. The origin of this difference is not clear at present. "Wind effects" can be excluded, since weaker winds – expected at lower metallicity – should lead to bluer SEDs and colors (although the effect is small in the optical, see above discussion), which is the opposite of what we see.

Such a change in the intrinsic $B-V$ colors of standard O stars[5] (at least −0.28 instead of −0.32) has important consequences for the distance determination of OB associations and young clusters. An increase of 0.04 mag in $(B-V)_0$ translates to a decrease in $E(B-V)$ by the same amount, which then implies a reduction of A_V by ∼0.124 mag (adopting $R_V = 3.1$). This means that the distance modulus is increased by the same amount. For clusters such as Tr16 in the Carina region (e.g. DeGioia et al. 2001), this is equivalent to an increase of the distance by 5.5%.

[5] We again stress that $(B-V)_0$ bluer than −0.28 can be obtained in atmosphere models if large gravities ($\log g \gtrsim 4.25$) are encountered, but such gravities are not typical of normal O stars.

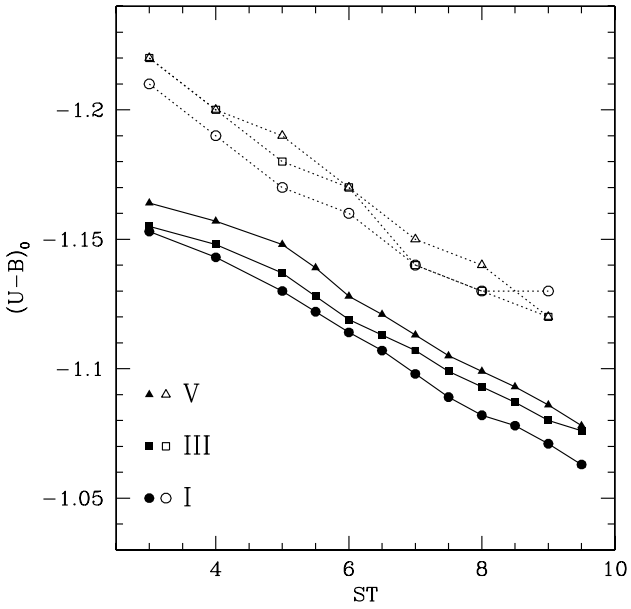

Fig. 6. $(U-B)$ intrinsic colors as a function of spectral type for the present work (solid symbols) and from Schmidt-Kaler (1982). Triangles (squares, circles) are for dwarfs (giants, supergiants). See text for discussion.

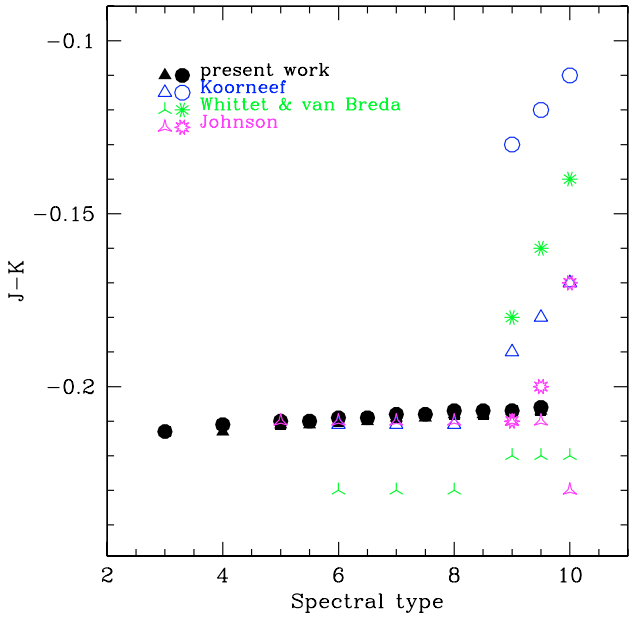

Fig. 7. $(J-K)_0$ as a function of spectral type for dwarfs (triangular shapes) and supergiants (circular shapes) from the present work, Koorneef (1983), Whittet & van Breda (1980) and Johnson (1966).

Inversely, if the distance is known, a reduction of $E(B-V)$ by 0.04 mag implies a luminosity that is lower by 0.05 dex for a given star.

Figure 6 shows the comparison between $(U-B)_0$ colors derived in the present study as a function of spectral type together with the values of Schmidt-Kaler (1982). Our values are systematically redder by ∼0.05 mag. Fitzgerald (1970) derived $(U-B)_0$ between −1.19 and −1.10 for dwarfs (lower values for early spectral types) and between −1.13 and −1.07 for O9–9.7 giants and supergiants, in marginal agreement with our values. Conti et al. (1986) found similar values (−1.12 to −1.07) for LMC stars and give $(U-B)_0 = -1.17$ for Galactic stars, again arguing that this value may be too blue (see discussion above). Finally, Fitzpatrick (1988) derived $(U-B)_0 = -1.04$ (resp. −1.08) for O3–6 (resp. O7–9.7) supergiants. Bessel et al. (1998) derived $(U-B)_0$ colors for O dwarfs using the ATLAS9 atmosphere models of Kurucz (1993, 1994). Their values range between −1.22 for the earliest O stars to −1.07 for the latest ones (see their Table 9). This is bluer than our results and similar to the results of Schmidt-Kaler (1982), but can be explained by the different $T_{\rm eff}$-scales used: adopting the cooler $T_{\rm eff} - ST$ relation of MSH05 compared to the relation of Crowther (1998) used by Bessel et al. (1998) translates into a shift of the $(U-B)_0 - ST$ relation towards earlier spectral types. Such a shift (of about one spectral sub type) reduces – although not completely – the difference between our relation and those of Bessel et al. (1998) and Schmidt-Kaler (1982), as seen in Fig. 6. The origin of the remaining difference is attributed to the use of more realistic models in our study.

On average, our $(U-B)_0$ colors are thus consistent with previous studies given the improvement in the model atmospheres.

3.2.2. Near-IR range

There are fewer studies of near infrared colors of O stars than of optical colors. The main ones are by Johnson (1966), Whittet & van Breda (1980), and Koorneef (1983). As for optical colors, Johnson (1966) used the method of the two-color diagram to derive intrinsic $(J-K)_0$. Whittet & van Breda (1980) proceeded differently and determined intrinsic near IR colors from a sample of 65 stars with low extinction (as deduced from optical colors). Their work was done in the Glass system (Glass 1974). Finally, Koorneef (1983) used a compilation of 127 standard stars in the Southern hemisphere to produce near-IR photometry and colors in the Johnson-Glass system (J and K in the Johnson system, H in the Glass system).

Figures 7 and 8 show the infrared $(J-K)_0$ and $(H-K)_0$ colors as a function of spectral type for the present work and previous studies by Johnson (1966), Whittet & van Breda (1980) and Koorneef (1983). The first interesting point to mention is that *our study covers the whole range of spectral types and luminosity classes*, which was not the case previously. Second, our IR colors are almost constant over the range of O stars: we do not find any significant variation in near-IR colors with spectral type or luminosity class.

The values of $(J-K)_0$ we find are similar to the ones by Johnson (1966). This is also true for the colors of Koorneef (1983), except for late spectral types for which our colors are bluer (by $\lesssim$0.1 mag), especially for supergiants. The values of Whittet & van Breda (1980) are a little bluer than ours for dwarfs and redder for supergiants.

As for $(H-K)_0$, there is reasonably good agreement with the values of Whittet & van Breda (1980), whereas Koorneef (1983) predicts redder colors than ours. However, the difference is rather small (∼0.05 mag). Blum et al. (2000) studied the stellar content of the HII region W42 and give intrinsic $H-K$ colors for ZAMS stars (see their Table 1). However, for O stars they adopt the value of Koorneef (1983).

The small differences we observe can be partly attributed to different photometric systems. However, the main conclusion is that, contrary to previous studies, we do not find any difference in near-IR colors between dwarfs and supergiants.

Overall, our results are an improvement on previous theoretical analysis due to the inclusion of line-blanketing and winds in the atmosphere models, as well as the use of a better $T_{\rm eff}$-scale.

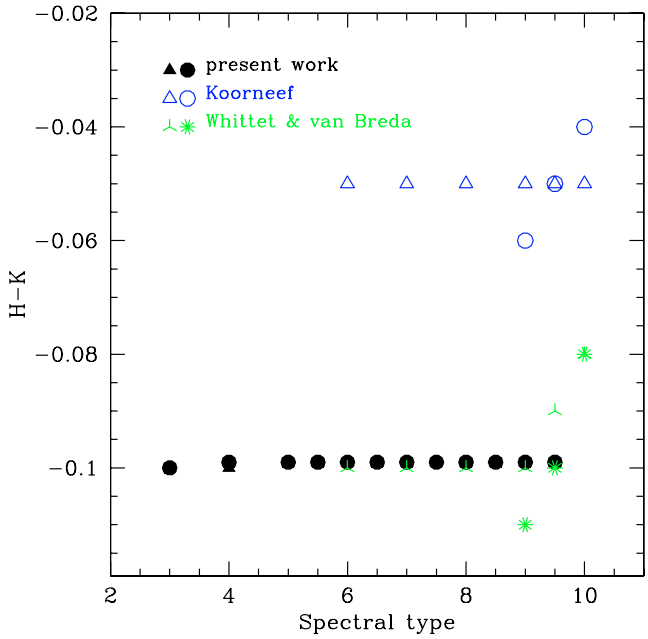

Fig. 8. $(H-K)_0$ as a function of spectral type for dwarfs (triangle shapes) and supergiants (circle shapes) from the present work, Koorneef (1983) and Whittet & van Breda (1980).

They present the advantage of covering the whole range of spectral types and luminosity classes of O stars in a consistent way. They also provide, for the first time, calibrations of bolometric corrections as a function of spectral type for the near infrared range.

4. Conclusion

We have derived calibrations of *UBVJHK* photometry for O stars as a function of effective temperature and spectral type using the recent grid of atmosphere models of Martins et al. (2005a). The *UBVJHK* photometry was computed as in Bessel et al. (1998), using the system of Bessel & Brett (1988, near IR) and Bessel (1990, optical).

We provide the first calibrations of near-IR photometry, including bolometric corrections, covering the whole range of spectral types and luminosity classes of O stars. Infrared colors are almost constant, with $(H-K)_0$ found to be −0.10, slightly lower (0.05 mag) than the value in Koorneef (1983).

Optical photometry is consistent with recent studies. One exception is the minimum value of $(B-V)_0$ for standard O stars (i.e. with $\log g \lesssim 4.0$), which is found to be −0.28, slightly higher than previously accepted (−0.32). This is important when estimating reddening and distances of OB associations since an error of 0.04 mag in color excess amounts to an error of ∼0.1 mag in distance modulus (or ∼0.05 dex in luminosity).

These calibrations will be useful for studying young massive stars embedded in star forming regions and to better understand their formation process.

Acknowledgements. F.M. acknowledges support from the Alexander von Humboldt foundation. We thank an anonymous referee for her/his rapid answer.

References

Abbott, D. C., & Hummer, D. G. 1985, ApJ, 294, 286
Bessel, M. S. 1990, PASP, 102, 1181
Bessel, M. S., & Brett, J. M. 1988, PASP, 100, 1134
Bessel, M. S., Castelli, F., & Plez, B. 1998, A&A, 333, 231
Bik, A., Kaper, L., Hanson, M. M., & Smits, M. 2005, A&A, 440, 121
Blum, R. D., Conti, P. S., & Damineli, A. 2000, ApJ, 119, 1860
Bonnell, I. A., Bate, M. R., & Zinnecker, H. 1998, MNRAS, 298, 93
Bouret, J. C., Lanz, T., Hillier, D. J., et al. 2003, ApJ, 595, 1182
Conti, P. S., Garmany, C. D., & Massey, P. 1985, ApJ, 92, 48
Crowther, P. A. 1998, in Fundamental Stellar Properties, ed. T. R. Bedding, A. J., Booth, & J. Davis (Kluwer, Dordrecht), IAU Symp., 189, 137
Crowther, P. A., & Conti, P. S. 2003, MNRAS, 355, 899
Crowther, P. A., Hillier, D. J., Evans, C. J., et al. 2002, ApJ, 579, 774
DeGioia-Eastwood, K., Throop, H., & Walker, G. 2001, ApJ, 549, 578
Fitzgerald, M. P. 1970, A&A, 4, 234
Fitzpatrick, E. L. 1988, ApJ, 335, 703
Gabler, R., Gabler, A., Kudritzki, R. P., Puls, J., & Pauldrach, A. W. A. 1989, A&A, 226, 162
Glass, I. S. 1974, Monthly Notes of the Astronomical Society of South Africa, 33, 53
Hanson, M. M., Howarth, I. D., & Conti, P. S. 1997, ApJ, 489, 698
Hillier, D. J., & Miller, D. L. 1998, ApJ, 497, 407
Hillier, D. J., Lanz, T., Heap, S. R., et al. 2003, ApJ, 588, 1039
IAU 1999, in Trans. IAU, Vol. XXIII B, ed. Andersen J., 141
Kennicutt, R. C. Jr. 1998, ARA&A, 36, 189
Krumbolz, M. R., Klein, R. I., & McKee, C. F. 2005 [arXiv:astro-ph/0510432]
Johnson, H. L. 1963, Basic Astronomical Data, ed. K. A. Strand (Chicago: University of Chicago Press), 214
Johnson, H. L. 1966, ARA&A, 4, 193
Koorneef, J. 1983, A&A, 128, 84
Kurucz, R. L. 1979, ApJS, 40, 1
Kurucz, R. L. 1993, CD-ROM No. 13
Kurucz, R. L. 1994, CD-ROM No. 14
Lamers, H. J. G. L. M., & Cassinelli, J. P. 1999, Introduction to stellar winds (Cambridge University Press)
Martins, F., Schaerer, D., Hillier, D. J., & Heydari-Malayeri, M. 2004, A&A, 420, 1087
Martins, F., Schaerer, D., & Hillier, D. J. 2005a, A&A, 436, 1049 (MSH05)
Martins, F., Schaerer, D., Hillier, D. J., et al. 2005b, A&A, 441, 735
Massey, P., Bresolin, F., Kudritzki, R. P., Puls, J., & Pauldrach, A. W. A. 2004, ApJ, 608, 1001
Mokiem, R. M., Martín-Hernández, N. L., Lenorzer, A., de Koter, A., & Tielens, A. G. G. M. 2004, A&A, 419, 319
Niemela, V. S., Morrell, N. I., Fernandez Lajus, et al. 2006, MNRAS, 367, 1450
Repolust, T., Puls, J., & Herrero, A. 2004, A&A, 415, 349
Russeil, D., Adami, C., Amram, P., et al. 2005, A&A, 429, 497
Schaller, G., Schaerer, D., Meynet, G., & Maeder, A. 1992, A&AS, 96, 269
Schmidt-Kaler, T. 1982, in Landoldt-Börnstein, New Seriesm Group, VI, ed. K. Schaifers, & H. H. Voigt (Berlin: Springer-Verlag), 2, 1
Vacca, W. D., Garmany, C. D., & Shull, J. M. 1996, ApJ, 460, 914
Whittet, D. C. B., & van Breda, I. G. 1980, MNRAS, 192, 467
Yorke, H. W., & Sonnhalter, C. 2002, ApJ, 569, 846